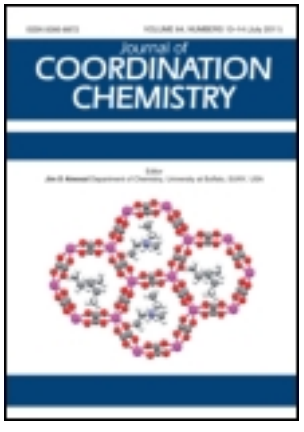

Journal of Coordination Chemistry
Publication details, including instructions for authors and subscription information:
http://www.tandfonline.com/loi/gcoo20

Synthesis, spectroscopic properties, and antimicrobial activity of some new 5-phenylazo-6-aminouracil-vanadyl complexes

Akmal S. Gaballa [a], Said M. Teleb [b], Mohsen S. Asker [c], Ergin Yalçin [d] & Zeynel Seferoğlu [d]

[a] Faculty of Specific Education, Zagazig University, Zagazig, Egypt

[b] Chemistry Department, Faculty of Science, Zagazig University, Zagazig, Egypt

[c] Microbial Biotechnology Department, National Research Center, P.O. 12622, Cairo, Egypt

[d] Faculty of Science-Arts, Department of Chemistry, Gazi University, 06500 Teknikokullar, Ankara, Turkey

Published online: 23 Nov 2011.

To cite this article: Akmal S. Gaballa, Said M. Teleb, Mohsen S. Asker, Ergin Yalçin & Zeynel Seferoğlu (2011) Synthesis, spectroscopic properties, and antimicrobial activity of some new 5-phenylazo-6-aminouracil-vanadyl complexes, Journal of Coordination Chemistry, 64:24, 4225-4243, DOI: 10.1080/00958972.2011.637554

To link to this article: http://dx.doi.org/10.1080/00958972.2011.637554

Journal of Coordination Chemistry
Vol. 64, No. 24, 20 December 2011, 4225–4243

Synthesis, spectroscopic properties, and antimicrobial activity of some new 5-phenylazo-6-aminouracil-vanadyl complexes

AKMAL S. GABALLA*†, SAID M. TELEB‡, MOHSEN S. ASKER§, ERGIN YALÇIN¶ and ZEYNEL SEFEROĞLU¶

†Faculty of Specific Education, Zagazig University, Zagazig, Egypt
‡Chemistry Department, Faculty of Science, Zagazig University, Zagazig, Egypt
§Microbial Biotechnology Department, National Research Center, P.O. 12622, Cairo, Egypt
¶Faculty of Science-Arts, Department of Chemistry, Gazi University, 06500 Teknikokullar, Ankara, Turkey

(*Received 21 August 2011; in final form 17 October 2011*)

Six complexes, $[VO(L^1\text{-}H)_2]\cdot 5H_2O$ (**1**), $[VO(OH)(L^{2,3}\text{–}H)(H_2O)]\cdot H_2O$ (**2**,**3**), $[VO(OH)(L^{4,5}\text{–}H)(H_2O)]\cdot H_2O$ (**4**,**5**), $[VO(OH)(L^{6}\text{–}H)(H_2O)]\cdot H_2O$ (**6**), were prepared by reacting different derivatives of 5-phenylazo-6-aminouracil ligands with $VOSO_4\cdot 5H_2O$. The infrared and ^1H NMR spectra of the complexes have been assigned. Thermogravimetric analyses (TG, DTG) were also carried out. The data agree quite well with the proposed structures and show that the complexes were finally decomposed to the corresponding divanadium pentoxide. The ligands and their vanadyl complexes were screened for antimicrobial activities by the agar-well diffusion technique using DMSO as solvent. The minimum inhibitory concentration (*MIC*) values for **1**–**4** and **6** were calculated at 30°C for 24–48 h. The activity data show that the complexes are more potent antimicrobials than the parent ligands.

Keywords: 5-Phenylazo-6-aminouracils-VO^{2+} complexes; IR; Thermal analysis; ^1H NMR; Antimicrobial activity

1. Introduction

A big branch of dyestuffs is the pyrimidine dyes which are used as hypnotic drugs for the nervous system, in detecting cancer, as chemotherapeutic agents, and are involved in the structure of nucleic acids in living cells [1–4]. Some pyrimidine derivatives have biological and pharmacological properties [5–8]. Uracil is a very important class of pyrimidine that has different medicinal, biological, and industrial applications [9–13] as well as in azo compound syntheses [14, 15]. Uracils have important applications in synthesis and its derivatives can be used as coupling components in the dye industry. Medicinal uses and applications of metal complexes are of increasing clinical and commercial importance [16–26]. Masoud *et al*. published a series of papers on the syntheses of uracil derivative-metal complexes and their biological applications [27–32].

*Corresponding author. Email: akmalsg@yahoo.com; akmalsg@hotmail.com

Journal of Coordination Chemistry
ISSN 0095-8972 print/ISSN 1029-0389 online
http://dx.doi.org/10.1080/00958972.2011.637554

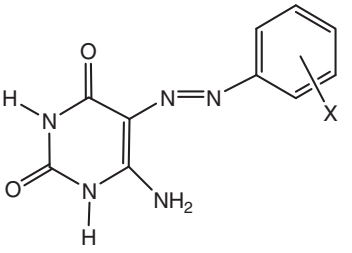

Figure 1. Structure of 5-phenylazo-6-aminouracils.

The role of vanadium in biological systems [33], such as discovery of the insulin-like properties of vanadate ions, spurred research into the clinical use of vanadium compounds as insulin mimics [34]. This work deals with the preparation and investigation of 5-phenylazo-6-aminouracil complexes with vanadyl ions. We investigate the effect of different derivatives (electron-donating and -accepting groups in m- and p-positions of 5-phenylazo) upon the mode of chelation of 5-phenylazo-6-aminouracils (figure 1) and the type of bonding and structures of the obtained complexes as well as their thermal behavior. Infrared and ^{1}H NMR spectra were assigned along with the thermal properties of vanadyl complexes. Also, the complexes were screened for their antimicrobial activities and mode of action.

2. Experimental

2.1. *Materials and spectral measurements*

All chemicals used were Analar, or of high grade. All organic compounds were prepared by the usual diazotization process [15].

Elemental analyses were carried out in the microanalysis unit of Cairo University, Egypt, using CHNS-932 (LECO) and Vario EL elemental analyzers. Vanadium content and water percentage were determined by thermogravimetric techniques [35]. The results obtained are in agreement with those calculated for the proposed formulas. Molar conductances of the complexes (10^{-3} mol L^{-1}) in DMSO were measured at room temperature using a 4310 conductivity meter. Thermal analyses (TG, DTG) were carried out using a Shimadzu TGA-50 H computerized thermal analysis system. The system includes a program which processes data from the thermal analyzer with the ChromotPac C-R3A. The rate of heating of the samples was kept at 10°C min^{-1}. Sample masses of 1.342, 1.673, and 1.899 mg for **1**, **2,** and **4**, respectively, were analyzed under N_2 flow at 20 mL min^{-1}. α-Alumina powder was used as DTA standard material. Infrared spectra of some reactants and the obtained complexes as well as their thermal products were recorded from KBr discs using a Perkin-Elmer 1430 Infrared Spectrophotometer. ^{1}H NMR spectra were recorded on a Varian spectrophotometer Gemini 200 operating at 200 MHz using DMSO-d_6 as solvent and TMS as internal reference.

2.2. *Synthesis of the vanadyl complexes*

A solution (30 mL, 1.10 mmol; 1:1 MeOH:NH_4OH) of the respective ligand was added to 10 mL, 0.50 mmol (1:1 H_2O:MeOH) of vanadyl(IV) sulfate, $VOSO_4 \cdot 5H_2O$. The reaction mixtures were stirred for 5–6 h and left overnight. The obtained precipitates were removed by filtration, washed several times with few drops of water, MeOH (3×1 mL), followed by Et_2O (3×1 mL). Finally, all the obtained complexes were dried under vacuum over P_4O_{10}.

[VO(L[1]-H)$_2$]·5H$_2$O (**1**): Yield: 323.0 mg (91.31%). Color: yellow. Anal. Found (Calcd for $C_{22}H_{28}N_{10}O_{14}V$, 707.46): C, 37.56 (37.35); H, 4.20 (3.99); N, 19.86 (19.80); V, 7.10 (7.20).

[VO(OH)(L[2]−H)(H$_2$O)]·H$_2$O (**2**): Yield: 190.0 mg (96.16%). Color: yellow. Anal. Found (Calcd for $C_{10}H_{12}N_6O_8V$, 395.18): C, 30.56 (30.39); H, 3.30 (3.06); N, 21.86 (21.27); V, 12.11 (12.89).

[VO(OH)(L[3]−H)(H$_2$O)]·H$_2$O (**3**): Yield: 180.0 mg (91.09%). Color: red. Anal. Found (Calcd for $C_{10}H_{12}N_6O_8V$, 395.18): C, 30.56 (30.39); H, 3.30 (3.06); N, 21.86 (21.27); V, 12.11 (12.89).

[VO(OH)(L[4]−H)(H$_2$O)]·H$_2$O (**4**): Yield: 140.0 mg (76.88%). Color: yellow. Anal. Found (Calcd for $C_{11}H_{15}N_5O_6V$, 364.21): C, 36.59 (36.28); H, 4.20 (4.15); N, 19.49 (19.23); V, 12.90 (13.99).

[VO(OH)(L[5]−H)(H$_2$O)]·H$_2$O (**5**): Yield: 158.0 mg (86.76%). Color: yellow. Anal. Found (Calcd for $C_{11}H_{15}N_5O_6V$, 364.21): C, 36.67 (36.28); H, 4.33 (4.15); N, 19.38 (19.23); V, 13.42 (13.99).

[VO(OH)(L[6]−H)(H$_2$O)]·H$_2$O (**6**): Yield: 162.0 mg (82.26%). Color: orange. Anal. Found (Calcd for $C_{12}H_{15}N_5O_7V$, 392.22): C, 36.89 (36.75); H, 4.02 (3.85); N, 18.10 (17.86); V, 12.61 (12.99).

2.3. *Antimicrobial activity*

The ligands and corresponding complexes were evaluated for their *in-vitro* antibacterial activity against *Bacillus subtilis* NRRL B-94, *Streptococcus aureus* NRRL B-313, *Escherichia coli* NRRL B-3703, and *Pseudomonas aeruginosa* NRRl B-32 and antifungal activity against *Aspergillus niger* NRRL 599, *Aspergillus fluves* NRC, *Saccharomyces cervisiea* NRC, and *Candida albicans* NRRL 477 by the agar-well diffusion method [36]. The studied bacteria and fungi were incubated into Nutrient Broth for 24 h and Malt-Extract Broth for 48 h, respectively. In this method, Nutrient agar for bacteria and Malt-Extract agar sterilized in a flask and cooled to 50°C was distributed (50 mL) to sterilized Petri dishes (15 cm in diameter) after injecting 0.1 mL cultures of bacterium or fungus, prepared as mentioned above and allowed to solidify. The dilution plate method was used to enumerate microorganisms (10^5 Cells mL^{-1}) for 24 h [37, 38]. By using a sterilized proper tube (6 mm diameter), wells were dug in the culture plates. Ligands or complexes dissolved in DMSO were added (100 µmol mL^{-1}) to these wells. The Petri dishes were left at 4°C for 2 h and then the plates were incubated at 30°C for bacteria (18–24 h) and (72 h) for fungi. At the end of the period, inhibition zones formed on the medium were evaluated as millimeters (mm) diameter.

The control samples were DMSO only. The antimicrobial tests were calculated as a mean of three replicates and the SD was calculated using the software SPSS, version 10 (SPSS, Richmond, USA).

2.4. *Determination of minimal inhibitory concentration (MIC)*

Nutrient and Malt-Extract agar are employed as basal medium for the growth of bacteria and fungi, respectively, during the test of **1**, **2**, **3**, **4,** and **6**. The culture medium (20 mL) was poured into Petri dishes (9 mm in diameter) and maintained at 45°C until the samples were incorporated into the agar. The samples were added as 1 mL using an automatic micropipette while constantly stirring to assure a uniform distribution. Each sample was tested at 25, 50, 75, 100, 125, 150, 175, and 200 μmol mL^{-1} in DMSO. The different bacterial strains were layered to place 30 μL over the surface of the solidified culture medium containing a sample. After the bacteria were absorbed into the agar, the plates were incubated at 30°C for 24–48 h. Bacterial growth was monitored visually and the MIC was determined [39, 40].

2.5. *Effect of the antimicrobial agent on protein and nucleic acids*

The effect of different concentrations of **1** on the growth rate and some biochemical activities was studied. Immediately after incubating the flasks with *B. Subtilis* NRRL B-94, cells were harvested during the middle logarithmic phase; the active compound was applied in a concentration of the 1/8, 1/4, and 1/2 MIC in three replicates. Subsequently, the flasks were shaken using a rotary shaker at 120 rpm at 30°C. Samples were withdrawn at the onset of the experiment and after incubation periods of 10, 30, 50, 70, 90, 120, 150, and 180 min. The bacterial cells were subjected to the following determinations: acid soluble phosphorus compounds, total lipids, total protein, and nucleic acid [41–46].

3. Results and discussion

3.1. *Synthesis of the vanadyl complexes*

Vanadyl complexes **1**–**6** were obtained during the reaction of vanadyl(IV) sulfate, $VOSO_4 \cdot 5H_2O$ with 5-phenylazo-6-aminouracils ($\mathbf{L^1}$–$\mathbf{L^6}$). The complexes were obtained in good yields (76–96%). The structures of complexes were verified by microanalyses, spectroscopic methods, and confirmed by thermal analysis (TG, DTG). The V content was determined by the gravimetric procedure [35]. The VO^{2+} complexes are 1:1 stoichiometry except for **1**, where it is 1:2. The 5-phenylazo-6-aminouracil ligands under investigation may exist in five tautomeric forms as shown in scheme 1. $\mathbf{L^3}$ did not show the tautomeric hydrazone peak and $\mathbf{L^{1-6}}$ showed the hydrazone-imine form [15].

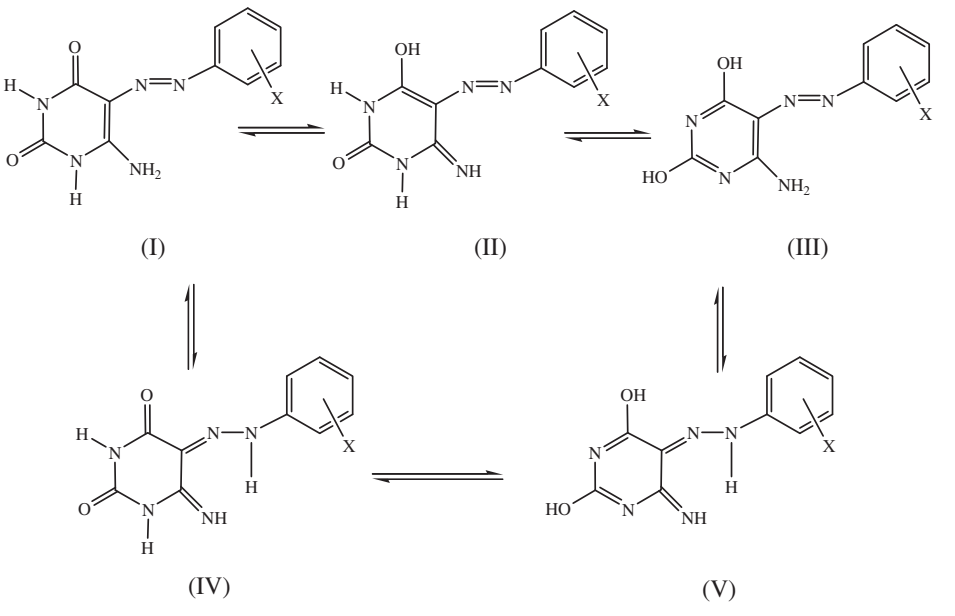

Ligand	L^1	L^2	L^3	L^4	L^5	L^6
X	*p*-COOH	*m*-NO_2	*p*-NO_2	*m*-CH_3	*p*-CH_3	*p*-$COCH_3$

Scheme 1. Tautomeric forms of 5-phenylazo-6-aminouracil derivatives.

3.2. *Conductance*

The molar conductivities (Λm) in DMSO at 25°C are in the range 2.44–5.13 $Ohm^{-1}\,cm^2\,mol^{-1}$, indicating the presence of non-electrolytes [47, 48].

3.3. *Vibrational spectra*

3.3.1. $[VO(L^1\text{-}H)_2]\cdot 5H_2O$ (1). The IR spectrum of **1**, as summarized in table 1, shows the following features. Broad bands at 3416 and 3410 cm^{-1} in 5-(4-carboxyphenylazo)-6-aminouracil, $\mathbf{L^1}$, and its vanadyl complex (**1**) are due to $\nu(-NH_2)$ and $\nu(O-H)$ of water with hydrogen bonds of the type N–H···O or N–H···N [28, 29, 49–51]. The observed band at 3166 cm^{-1} corresponding to $\nu(N-H)$ in the spectrum of $\mathbf{L^1}$ is strongly affected on complexation to VO^{2+} with only one band at 3211 cm^{-1} due to V–O interaction [50]. Absorptions of free carboxyl, $\nu(C=O)$, observed at 1729 and 1708 cm^{-1} in the spectrum of free $\mathbf{L^1}$ are red shifted on complexation to VO^{2+} with different degrees. Only one strong absorption is observed at 1717 cm^{-1}. The strong absorption of the aromatic ketones, $\nu(C=O)$, at 1631 cm^{-1} is slightly blue shifted on complexation and observed at 1641 cm^{-1}, typical of V–O bonding to carboxyl [51]. The absorption at 1416 cm^{-1} due to $\nu(N=N)$ of $\mathbf{L^1}$ is observed in the same region on complexation (1414 cm^{-1}), indicating the absence of V–azo bonding [49–53]. The $\nu(V=O)$ is very strong at 918 and 851 cm^{-1}. In the lower frequency spectral region

Table 1. IR frequencies (cm^{-1}) and assignments for 5-(4-carboxphenylazo)-6-aminouracil, $\mathbf{L^1}$, and **1**.

Wavenumbers[a] (cm^1)		
$\mathbf{L^1}$	**1**	Assignments[b]
3416, mbr	3410, mbr	ν(O–H); H_2O $\nu(-NH_2)$
3166, mbr	3211, s	ν(N–H)
3013–2800, br	2971, s	ν(C–H)
	2802, s	
1729, s	-	ν(C=O); free COOH
1708, sh	1717, s	ν(C=O); COO–V
1631, vs	1641, s	ν(C=O), keto groups $\delta(H_2O)$
1543, s	1536, s	ν(C=N)
1481, m	1414, vs	ν(N=N)
1416, m	1380, m	C–H deformation ν(C=C)
1256, vs	1256, w	ν(C–O); COO^-
1214, m		ν(C–N)
1172, w		ν(C–C)
1102, w	918, s	C–H bend
	851, m	ν(V=O)
	769, m	δ(COC)
	662, s	ν(V–O)
	529,w	ν(V–O)

[a]m, medium; s, strong; vs, very strong; w, weak; br, broad.
[b]ν, stretching; s, symmetric; as, asymmetric; δ, bending.

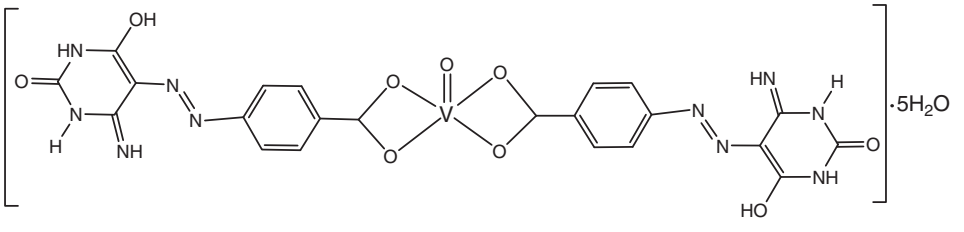

Figure 2. Structure of **1**.

bands for symmetric and asymmetric vibrational motion of ν(V–O), two bands are observed at 662 and 529 cm^{-1} [50]. The proposed structure of **1** is shown in figure 2.

3.3.2. $[VO(OH)(L^{2-5}-H)(H_2O)] \cdot H_2O$ (2–5). IR spectra of **2** and **3**, table 2, show the following features. Medium to very strong bands at 3224 and 3433 cm^{-1} are assigned to ν(O–H) of coordinated H_2O and OH^-. The ν(N–H) of imides in the uracil ring at 3160 and 3127 cm^{-1} in spectra of $\mathbf{L^2}$ and $\mathbf{L^3}$ are blue shifted to 3181 and 3171 in spectra of **2** and **3**, respectively. These data indicate the absence of imide, V–N interaction, and the presence of imine, V–N interaction. The ν(C=O) bands of aromatic ketones in free $\mathbf{L^2}$ and $\mathbf{L^3}$ at 1727 and 1737 cm^{-1}, respectively, slightly blue shift on complexation to VO^{2+}

Table 2. IR frequencies (cm^{-1}) and assignments for $\mathbf{L^{2-5}}$ and their corresponding complexes (**2**–**5**).

Wavenumbers[a] (cm^{1})								
L^2	L^3	L^4	L^5	2	3	4	5	Assignments[b]
						3531, s		ν(O–H); OH^-
3422, m	3428, br			3424,mbr	3433,vs,br			ν(O–H); H_2O
3358, m		3435, w	3447, w	3400,sh		3469, m	3440, m	ν ($-NH_2$)
						3224, vs	3220, sh	ν (–NH)
3160, m	3127, s	3162, s	3170,s	3181,s	3172, s,br	3170, sh	3194, s	
3108, m	3024, m	3031, m	3024,s	3112, sh	3050, sh	3025, s	3019, s	ν (Ar C–H)
2995, s		–	3018,sh	2973, s	2927, s		2925, s	
		2812, m	2921, m			2820, m	2798, m	ν (Aliph. C–H)
		–	1759, s				1758, s	
1727, vs	1737, s	1715, vs	1715, vs	1740, s	1740, s	1730, vs	1715, sh	ν (C=O)
1689, vs		1672, s						
1649, vs	1636, s	1630, vs		1632, vs	1633, vs	1633, vs	1629, vs	$\delta(H_2O)$
1522, vs	1554, m	1544, vs	1530, s	1524, s	1545, m	1533, s	1532, m	ν (C=N)
1464, m	1501, s				1504, s			
1431, s	1470, m	1460, s	1457, m	1413, vs	1417, s	1411, vs		ν (N=N)
1401, s								
1348, vs	1344, vs	1413, s	1390, m	1351, vs	1337, vs			
1272, m	1289, m		1342, m	1274, m	1248, m			ν (C=C)
1210, m	1244, s	1299, m	1266, w	1209, m	1211, m			C–H
	1208, m	1267, s	1230, m		1099, m			deformation
		1232, m	1128, m					
				911, s	900, m	919, s	919, m	ν (V=O)
				815, m	852, m	860, w	819, m	
817, m	856, m	854, w	757, m	739, m	752, m	828, w	751, m	δ(COC)
757, m	750, w	768, w	672, m	663, m	688, m	675, m	660, sh	ν (V–O)
		687, w				664, s	636, m	
				518, m	519, w	541, m	528, m	ν (V–O)
						505, m		
				450, w	433, w	421, w	418, vw	ν (V–N)

[a]m, medium; s, strong; vs, very strong; w, weak; br, broad; sh, shoulder.
[b]ν, stretching; s, symmetric; as, asymmetric; δ, bending.

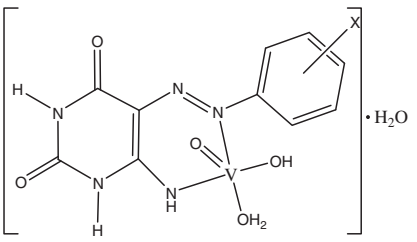

Complex	2	3	4	5
X	*m*-NO_2	*p*-NO_2	*m*-CH_3	*p*-CH_3

Figure 3. Structure of **2**–**5**.

(1740 cm^{-1}) for both complexes. These data verify the absence of V–O interaction. The observed strong to medium bands at 1431 and 1470 cm^{-1} due to ν(N=N) of free $\mathbf{L^2}$ and $\mathbf{L^3}$ red shift on complexation to 1413 and 1417 cm^{-1}, respectively, indicating the presence of V–azo bonding [49–53]. In IR spectra of **4** and **5** (table 2), similar features are observed for both complexes. The observed strong to medium bands at 1460 and 1457 cm^{-1} due to ν(N=N) of free $\mathbf{L^4}$ and $\mathbf{L^5}$ red shift on complexation to 1411 cm^{-1}, indicating the presence of V–azo bonding [50–53].

The ν(V=O) is observed between 919 and 819 cm^{-1} for **2**–**5**. For ν(V–O), two bands are observed at 663 and 518 cm^{-1} for **2**, 688 and 519 cm^{-1} for **3,** and between 675 and 505 cm^{-1} for **4** and **5** [50]. These data are from V–O interaction of H_2O or OH^- groups. The ν(V−N) band is observed at 450, 433, 421, and 418 cm^{-1} in spectra of **2**–**5**, respectively. The proposed structures for **2**–**5** are shown in figure 3.

3.3.3. [VO(OH)(L^6−H)(H_2O)] · H_2O (6). The infrared spectrum of the V–L^6 complex [VO(OH)(L^6−H)(H_2O)] · H_2O (**6**) shows two bands at 3568 and 3496 cm^{-1}, due to ν(O–H) of coordinated OH^- or H_2O in the complex [50, 54] (table 3). The band at 3331 cm^{-1} is due to ν(N−H) of coordinated 5-(4-acetylphenylazo)-6-aminouracil and in the same region as free ligand (3326 cm^{-1}). The ν(−NH) of aminouracil ring in free $\mathbf{L^6}$ at 3159 cm^{-1} is strongly affected on complexation to VO^{2+} with the presence of only one band at higher value, 3198 cm^{-1}. Thus, the imino nitrogen, N3, and carbonyl oxygen, C4=O, are chelating sites [50–53]. Bands at 1718, 1705, 1693, 1630, and 1593 cm^{-1} due to different ν(C=O) in free $\mathbf{L^6}$ (carbonyl of acetyl and aromatic ketones) are strongly affected on complexation with two bands observed at 1702 and 1649 cm^{-1}. The very strong 1649 cm^{-1} band was assigned to ν(C=O) of the coordinated aminouracil. The absorption at 1475 cm^{-1} due to ν(N=N) of the free ligand, $\mathbf{L^6}$, is observed in the same region on complexation (1476 cm^{-1}), suggesting the absence of V–azo bonding [50–53]. The vibrational modes of ν(C–C), ν(C–N), δ(CH), δ(OH), and δ(NH) suggest that the oxygen, O4, and nitrogen, N3, are centers for complexation [49, 52, 53]. The presence of bands at 653, 604, 531, and 459 cm^{-1} are due to ν(V–O) and ν(V–N), respectively [49–51], and the proposed structure is illustrated by figure 4.

Table 3. IR frequencies (cm^{-1}) and assignments for 5-(4-acetylphenylazo)-6-aminouracil, **L**[6], and **6**.

Wavenumbers[a] (cm^{1})		
L^6	**6**	Assignments[b]
	3568, m	ν(O−H); OH^-
	3496, m	ν(O−H); H_2O
3326, m	3331, m	$\nu(-NH_2)$
3159, m	3198, m	ν (−NH)
3012, m	3085, m	ν (Ar C−H)
	3009, m	
2800, m	2798, m	
		ν (Aliph. C−H)
1718, s	1702, s	ν (C=O)
1705, s		
1693, s		
1630, s		
1598, s		
	1649, vs	ν (C=O); CO−V
		$\delta(H_2O)$
1545, s	1542, s	ν (C=N)
1475, m	1476, m	ν (N=N)
		C−H deformation
1415, m	1415, s	ν (C=C)
		ν (C−N)
1358, m	1253, vs	
1220, vs		
1210, w		
1175, w	1174, w	ν (C−C), C−H bend
1140, w		and $\delta_r(H_2O)$
1090, w		δ(O−H); OH^-
	917, m	ν (V=O)
827, m	836, w	
		δ(COC)
	653, m	ν (V−O)
	604, w	ν (V−O)
	531, w	
	459, w	ν (V−N)
	414, m	δ(O=V−O)

[a]m, medium; s, strong; vs, very strong; w, weak; br, broad.
[b]ν, stretching; s, symmetric; as, asymmetric; δ, bending.

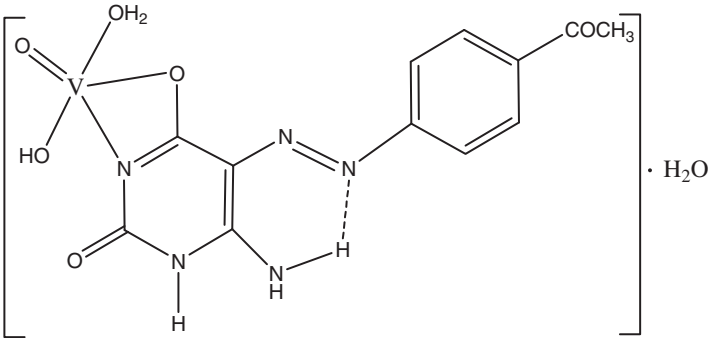

Figure 4. Structure of **6**.

3.4. *^{1}H NMR spectra*

3.4.1. $[VO(L^1\text{-}H)_2]\cdot 5H_2O$ (1). Deuterated DMSO provided adequate solubility [55] for recording ^{1}H NMR signals of $\mathbf{L^1}$ and **1** (table 4). Signals at 14.11 and 12.94 ppm corresponding to tautomeric hydrazone, –N*H*, and –COO*H* were not observed, confirming the coordination of $\mathbf{L^1}$ to VO^{2+} via carboxyl. Signals at 10.42 and 7.93 ppm are –N1*H* and tautomeric imine, –N*H*, respectively, in the expected region of the free ligand, $\mathbf{L^1}$, so the presence of form II (scheme 1) is assigned [15, 56–59]. Disappearance of –N3*H* (ligand at 11.00 ppm) and appearance of two new broad signals at 5.21 and 5.05 ppm could be assigned to –N3*H* and –OH_2. This low field shift might be attributed to hydrogen bonding between –N3*H* and –OH_2 in form II.

3.4.2. $[VO(OH)(L^{2-5}\text{–}H)(H_2O)]\cdot H_2O$ (2–5). There are some general features in ^{1}H NMR spectra of **2**–**5** (table 4). Broad signals corresponding to the tautomeric hydrazones observed in spectra of $\mathbf{L^2}$–$\mathbf{L^5}$ were not observed in the corresponding complexes. The protons of –N3*H* and N1*H* are observed in the expected region with very small differences in their chemical shifts. Broad signals of tautomeric imine protons were observed at 8.41, 8.20, 8.29, and 8.33 ppm for **2**–**5**, respectively. New broad signals at 3.49, 3.52, 5.04, and 5.00 ppm in **2**–**5**, respectively, are assigned to coordinated OH_2 and OH^- (see the ^{1}H NMR spectrum of **2**, figure 5). These observations confirm the coordination of 5-phenylazo-6-aminouracils, $\mathbf{L^2}$–$\mathbf{L^5}$ to VO^{2+} *via* nitrogens of deprotonated hydrazone and tautomeric imine. The other two coordination sites on VO^{2+} are occupied with OH^- and H_2O.

3.4.3. $[VO(OH)(L^6\text{–}H)(H_2O)]\cdot H_2O$ (6). Broad signals at 14.08, 11.04, and 7.94 ppm corresponding to tautomeric hydrazone, –N3*H*, and tautomeric imine protons in free $\mathbf{L^6}$ were not observed in the ^{1}H NMR spectrum of **6** (table 4). New broad signals are observed at 7.85 and 5.11 ppm corresponding to –NH_2 and O*H*, respectively, confirming the coordination of $\mathbf{L^6}$ to VO^{2+} *via* deprotonated N3 and carbonyl oxygen, C4=O. The signal of N1*H* is observed in the expected region at 10.44 and a new broad signal at 7.85 ppm corresponds to –N6H_2. So, the presence of form I is assigned [56–60]. The appearance of a new broad signal at 5.11 ppm is assigned to coordinated –O*H* and –OH_2 protons.

3.5. *Thermal analysis*

To confirm the proposed structures for the complexes, thermogravimetric analyses TGA and DTG are measured under nitrogen. The thermal data for **1**, **2,** and **4** are summarized in table 5. The decomposition reactions of $[VO(L^1\text{–}H)_2]\cdot 5H_2O$ (**1**) occur in five steps from 127°C to 406°C. The first step of decomposition proceeds with a weight loss of 13.50% at 127°C, associated with the loss of lattice water (calculated 12.43%). The second, third, fourth, and fifth steps of decomposition proceed at maximum temperatures of 182, 214, 365, and 406°C, respectively, attributed to the loss of $C_{22}H_{18}N_{10}O_{6.5}$ of $\mathbf{L^1}$. The total weight loss associated with these steps (75.03%) is in good agreement with the calculated value of 74.79%.

Table 4. ^{1}H NMR δ values (ppm) of **L**$^{1\text{-}6}$ and vanadyl complexes (**1**–**6**) in DMSO-d_6.

	Band assignments									
Compound	Tautomeric hydrazone, –NH	–COOH	–N3H	–NH	Tautomeric imine, –NH	–NH_2	4 H	H_2O and –NH	OH and H_2O	–CH_3 or –$COCH_3$
L^{1}	14.11, b	12.94, b	11.03, b	10.63, b	7.94, b		8.28, d	–		
							7.54, d	–		
1	–	–	–	10.42, b	7.93, b		7.63, b	5.21, b		
								5.05, b		
L^{2}	14.13, b		11.00, b	10.68, b	8.51, b	–	8.06–7.63, m		–	
2				10.44, b	8.41, b	–	8.03–7.70, m, b		3.49, b	
L^{3}			11.18, b	10.74, b		8.16, b	8.42, d		–	
							7.83, d			
3				10.54, b	8.20, b	–	8.40, d		3.52, b	
							7.86, d		–	
L^{4}	14.13, b		10.96, b	10.51, b	8.08, b		7.74–7.16, m			
4			10.89, b	10.47, b	8.29, b		7.30, b		5.04, b	2.57, s
L^{5}	14.18, b		11.06, b	10.64, b	8.28, b		7.71, d		–	2.58, s
							7.26, d			
5			10.93, b	10.41, b	8.33, b		7.42, b		5.00, b	2.56, s
L^{6}	14.08, b		11.04, b	10.66, b	7.94, b		8.21, d		–	2.60, s
							7.23, d			
6				10.44, b		7.85, b	7.45, b		5.11, vb	2.61, s

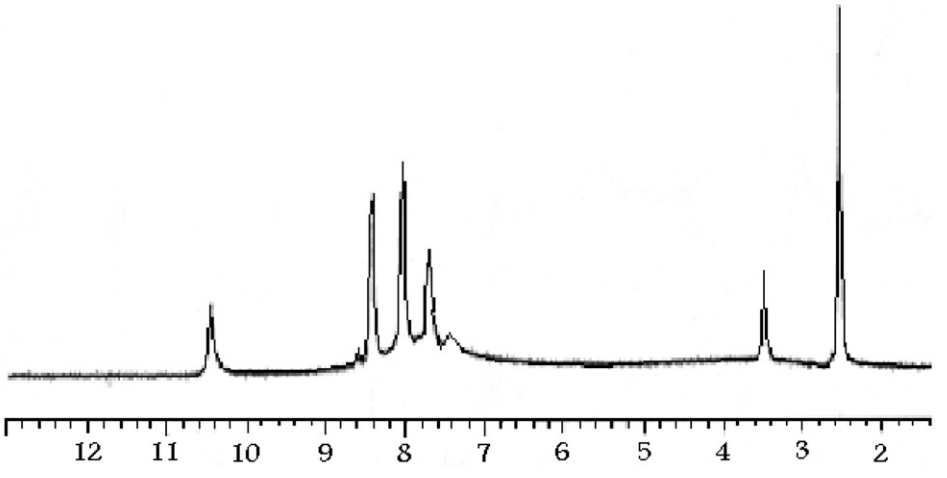

Figure 5. ^{1}H NMR spectrum of $[VO(OH)(L^{2}-H)(H_2O)]\cdot H_2O$ (**2**).

Table 5. Maximum temperature values for decomposition along with the species lost in each step of the decomposition of the complexes.

Complex	Decomposition	T_{max} (°C)	Lost species	% Weight loss	
				Found	Calcd
$[VO(L^{1}-H)_2]\cdot 5H_2O$ (**1**)	First step	127	$5H_2O$	13.50	12.43
	Second step	182			
	Third step	214			
	Fourth step	365			
	Fifth step	406	$C_{22}H_{18}N_{10}O_{6.5}$	75.03	74.79
	Total loss			88.53	87.22
	Residue		$VO_{2.5}$	11.47	12.78
$[VO(OH)(L^{2}-H)(H_2O)]\cdot H_2O$ (**2**)	First step	55	H_2O	5.20	4.56
	Second step	184	H_2O	4.90	4.56
	Third step	220			
	Fourth step	318			
	Fifth step	460	$C_{10}H_8N_6O_{3.5}$	65.68	67.87
	Total loss			75.78	76.99
	Residue		$VO_{2.5}$	24.22	23.01
$[VO(OH)(L^{4}-H)(H_2O)]\cdot H_2O$ (**4**)	First step	77	H_2O	5.00	4.95
	Second step	188	H_2O	5.00	4.95
	Third step	222			
	Fourth step	305			
	Fifth step	446	$C_{10}H_8N_6O_{3.5}$	65.94	65.13
	Total loss			75.94	75.03
	Residue		$VO_{2.5}$	24.06	24.97

Decomposition of $[VO(OH)(L^{2}-H)(H_2O)]\cdot H_2O$ (**2**) also occurred in five steps. Lattice water is lost at 55°C with 5.20% weight loss (calculated 4.56%). The second step of decomposition proceeded at 184°C, associated with the weight loss of 4.90% from the loss of one coordinated water molecule (calculated 4.56%). The third, fourth, and fifth degradation steps were observed as three consequent decomposition peaks at 220,

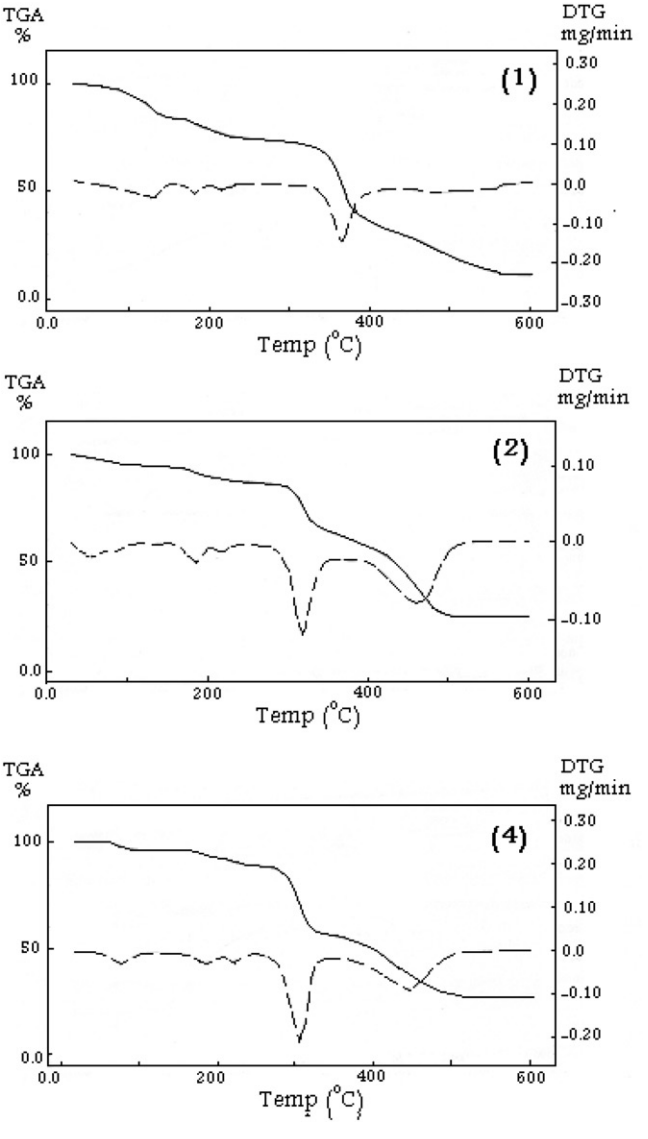

Figure 6. Thermogravimetric (TG) and derivative (DTG) of **1**, **2**, and **4**.

318, and 460°C. The total weight loss value for the three steps was 65.68% associated with the loss of $C_{10}H_8N_6O_{3.5}$ (coordinated ligand, $\mathbf{L^2}$), which agrees with the theoretical value of 67.87%.

The decomposition reactions of $[VO(OH)(L^4{-}H)(H_2O)]\cdot H_2O$ (**4**) occurred in five steps in a similar manner to **2** (table 5 and figure 6).

3.6. *Antimicrobial activity*

The new ligands and metal complexes were evaluated for *in vitro* antibacterial activity against *P. aeruginosa*, *E. coli*, *B. subtilis*, and *St. aureus* and *in vitro* antifungal activity

against *C. albicans*, *S. cervisiea*, *A. flavus*, and *A. niger* by using agar-well diffusion. The complexes are more toxic than the ligands. Complexes **1** and **6** are much more active as antimicrobial agents than the other complexes; **1** shows the highest antimicrobial activity against all microorganisms. The highest inhibition occurred for **1** against *P. aeruginosa* NRRl B-32 (as gram negative bacteria) (table 6). Most complexes have antifungal effect except **5**. Complex **1** showed the best activity against *P. aeruginosa* NRRl B-32 (22.66 ± 0.09 mm) and the lowest against *B. subtilis* NRRL B-94 (17.63 ± 0.03 mm). All complexes show antibacterial activities against *B. subtilis* NRRL B-94, *St. aureus* NRRL B-313, *P. aereuguinosa* NRRL B-32, and *E. coli* NRRL B-3703. Inhibition zone results were dependant on the type of ligand and the position of chelation with vanadyl [61, 62].

Antimicrobial activities are also reported as minimum inhibitory concentration (MIC) values, defined as the lowest concentration of an antimicrobial that visibly inhibits growth of the bacteria after overnight incubation. Minimum inhibitory concentrations (MIC) of $50.00\,\mu mol\,mL^{-1}$ were observed in all microorganisms tested except **2,** for which the MIC against *St. aureus* NRRL B-313, *B. subtilis* NRRL B-94, *A. flavus*, and *A. niger* NRRL599 was $150.00\,\mu mol\,mL^{-1}$. Complex **1** exhibited antimicrobial activities better than other complexes. The variation in the effectiveness of different complexes against different organisms depend either on differences in the permeability of the cells of the microbes or on difference in ribosome's of the microbes [63–65].

The impact of different concentrations of **1** on the biosynthesis of acid-soluble phosphorus, intracellular lipids, proteins, and nucleic acids (RNA and DNA) in the cells of *B. subtilis* NRRL B-94 was studied (figures 7–11). Complex **1** had a drastic effect on the biosynthesis of acid-soluble phosphorus, intracellular lipids, and proteins in cells of *B. Subtilis*. The complex affects the synthesis of DNA or RNA, or can bind to DNA or RNA so that their messages cannot be read. This complex is unselective, however, affecting animal and bacterial cells alike, and thus has no therapeutic applications. The mode of action involves the formation of hydrogen bonds through nitrogen in interference with the active contents of the cell constituents, resulting in interference with the normal cell process [65–68]. Inhibition growth may be due to the effect of the biosynthesis of phospholipids and proteins in cell membrane.

4. Conclusion

Different types of vanadyl-5-phenylazo-6-aminouracil complexes were synthesized by the reaction of 5-phenylazo-6-aminouracil ligands with VO^{2+} ions. When 5-(4-carboxyphenylazo)-6-aminouracil was used as ligand with the carboxyl, –COOH, in *p*-position of the benzene ring, coordination with VO^{2+} took place through carboxyl group and VO^{2+}–$\mathbf{L^1}$ was isolated with 1:2 molar ratio. Complexes **2**–**5** were isolated in 1:1, VO^{2+}–**L** molar ratios. The presence of electron-accepting, $-NO_2$ or electron donating, $-CH_3$ groups in *m*- or *p*-positions of the benzene ring have no effect on the chelating mode (**2**–**5**) and one type of bonding was observed. When the substituent was $-COCH_3$ at the *p*-position of the benzene ring, another type of coordination was observed in **6**. Similar thermal degradation was observed for **2** and **4**. Antibacterial and antifungal studies confirmed that ligands are biologically active and their vanadyl

Table 6. Antimicrobial activity of 5-phenylazo-6-aminouracil ligands and their vanadyl complexes (diameter of inhibition in mm).

	Diameter of inhibition zone (mm)							
	Bacteria				Fungus		Yeast	
	E. coli	*P. aeruginosa*	*St. aureus*	*B. subtilis*	*A. niger*	*A. flavus*	*S. cervisiea*	*C. albicans*
$VOSO_4$	16.12 ± 0.047	15.677 ± 0.047	16.43 ± 0.047	15.85 ± 0.049	16.62 ± 0.049	15.82 ± 0.140	16.54 ± 0.049	15.66 ± 0.047
L1	10.64 ± 0.094	11.35 ± 0.120	09.79 ± 0.093	12.30 ± 0.094	10.37 ± 0.096	10.65 ± 0.043	09.68 ± 0.047	09.48 ± 0.049
1	21.38 ± 0.198	22.66 ± 0.092	19.75 ± 0.079	17.63 ± 0.029	19.72 ± 0.096	17.86 ± 0.093	18.62 ± 0.091	19.23 ± 0.047
L2	07.68 ± 0.047	08.67 ± 0.069	07.34 ± 0.047	08.33 ± 0.029	07.71 ± 0.047	07.65 ± 0.091	07.88 ± 0.091	08.67 ± 0.049
2	15.82 ± 0.091	18.33 ± 0.097	17.67 ± 0.094	13.87 ± 0.049	15.28 ± 0.091	16.11 ± 0.093	13.40 ± 0.093	11.83 ± 0.049
L3	09.62 ± 0.041	08.38 ± 0.041	09.29 ± 0.043	10.12 ± 0.091	07.68 ± 0.045	09.77 ± 0.041	07.46 ± 0.047	06.87 ± 0.041
3	17.38 ± 0.047	14.76 ± 0.093	15.57 ± 0.091	17.22 ± 0.049	12.82 ± 0.049	13.27 ± 0.041	14.35 ± 0.094	13.91 ± 0.093
L4	09.88 ± 0.093	10.27 ± 0.049	08.86 ± 0.093	10.26 ± 0.094	12.41 ± 0.091	08.87 ± 0.049	09.93 ± 0.045	10.26 ± 0.049
4	16.85 ± 0.193	18.46 ± 0.091	15.67 ± 0.079	18.53 ± 0.095	16.87 ± 0.093	17.47 ± 0.043	14.75 ± 0.091	15.31 ± 0.049
L5	07.82 ± 0.049	08.00 ± 0.049	07.54 ± 0.041	07.83 ± 0.029	00.00 ± 0.000	00.00 ± 0.000	00.00 ± 0.000	00.00 ± 0.000
5	17.00 ± 0.093	19.35 ± 0.047	15.29 ± 0.049	15.85 ± 0.091	00.00 ± 0.000	00.00 ± 0.000	00.00 ± 0.000	00.00 ± 0.000
L6	08.65 ± 0.047	08.34 ± 0.043	07.85 ± 0.041	09.25 ± 0.029	07.22 ± 0.049	05.70 ± 0.043	07.00 ± 0.029	08.28 ± 0.041
6	19.33 ± 0.140	18.66 ± 0.095	17.84 ± 0.049	15.78 ± 0.091	15.75 ± 0.093	15.53 ± 0.140	16.00 ± 0.095	17.32 ± 0.094
R1	27.35 ± 0.198	28.65 ± 0.095	27.25 ± 0.91	25.30 ± 0.095	00.00 ± 0.000	00.00 ± 0.000	00.00 ± 0.000	00.00 ± 0.000
R2	00.00 ± 0.000	00.00 ± 0.000	00.00 ± 0.000	00.00 ± 0.000	25.60 ± 0.093	26.40 ± 0.046	28.00 ± 0.091	27.60 ± 0.080

Each value represents mean of sample ± SD for $n = 3$. Diameter of inhibition zone was measured as the clear area centered on the agar well containing the sample. Well with non-inhibition zone were recorded 0.00. R1 and R2 represent Ampicilin and Fluconazol, respectively.

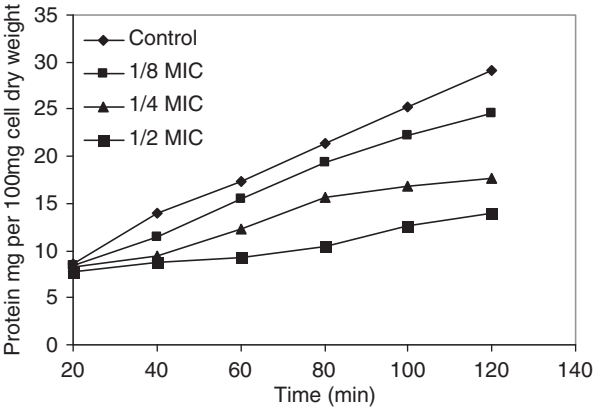

Figure 7. Effect of different concentrations of **1** on the biosynthesis of protein in cells of *B. subtilis* NRRL B-94.

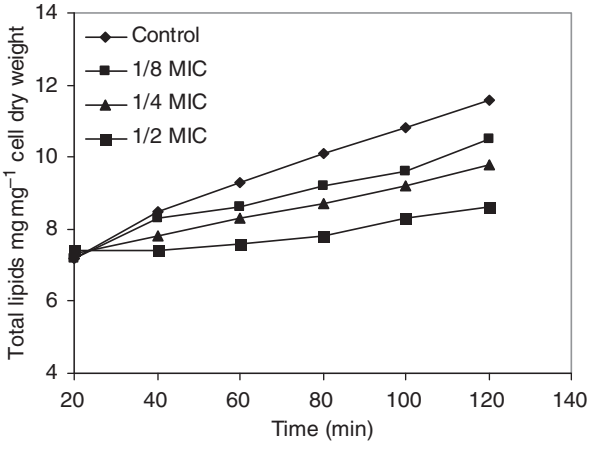

Figure 8. Effect of different concentration of **1** on total lipid content in cells of *B. subtilis* NRRL B-94.

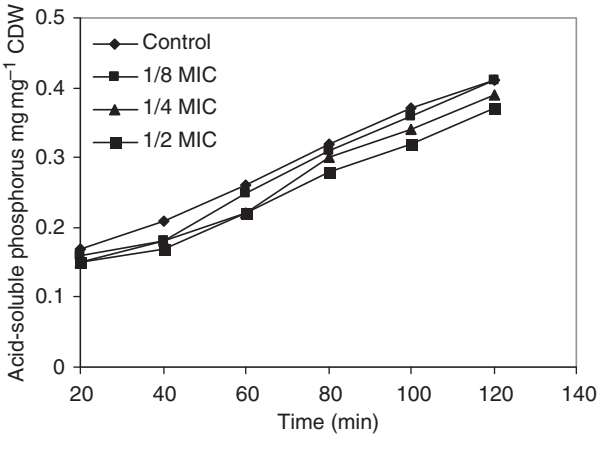

Figure 9. Effect of different concentrations of **1** on acid-soluble phosphorus content in cells of *B. subtilis* NRRL B-94.

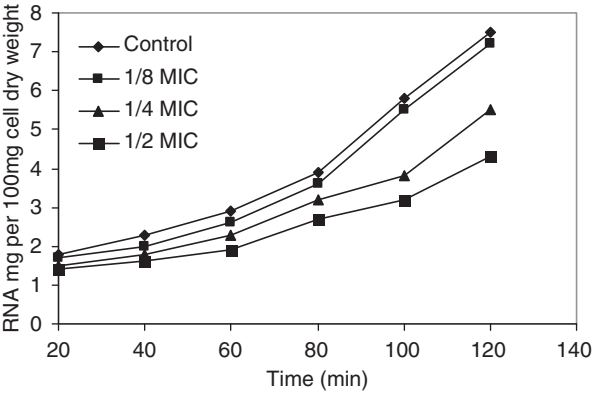

Figure 10. Effect of different concentrations of **1** on RNA content in cells of *B. subtilis* NRRL B-94.

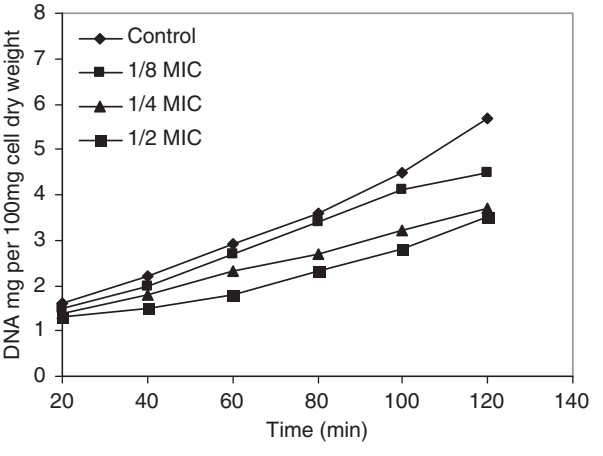

Figure 11. Effect of different concentrations of **1** on DNA content in cells of *B. subtilis* NRRL B-94.

complexes show enhanced activity. The same behavior has been observed on similar systems containing VO^{2+} [67, 68]. The examined complexes show significant differences for their antimicrobial activities in comparison with the corresponding free ligands.

Supplementary material

The table containing the minimum inhibition concentration (MIC, μmol mL^{-1}) of **1**, **2**, **3**, **4,** and **6** against some microorganisms has been deposited as a supplementary data.

Acknowledgments

The authors are very grateful to Zagazig University Research Fund for providing financial support (project no. 36K12/M3).

References

[1] J. Clayden, *Organic Chemistry*, 1st Edn, pp. 1345–1352, Oxford University Press, USA (2000).
[2] S. Pati, *The Chemistry of the Hydrazo, Azo and Azoxy Groups*, Part 1, Wiley, New York (1975).
[3] W.C. Cutting. *Handbook of Pharmacology*, 3rd Edn, Meredith Company, New York (1967).
[4] R.M. Izatt, J.H. Christensen, J.H. Rytting. *Chem. Rev.*, **72**, 439 (1972).
[5] H. Zeng, Z.P. Lin, A.C. Sartorelli. *Biochem. Pharmacol.*, **68**, 911 (2004).
[6] P. Sharma, N. Rane, V.K. Gurram. *Bioorg. Med. Chem. Lett.*, **14**, 4185 (2004).
[7] C.Q. Huang, K.M. Wilcoxen, D.M. Grigoriadis, J.R. McCarthy, C. Chen. *Bioorg. Med. Chem. Lett.*, **14**, 3943 (2004).
[8] T.P. West. *Microbiol. Res.*, **159**, 29 (2004).
[9] H. Wamhoff, J. Dzenis. *Adv. Heterocycl. Chem.*, **55**, 129 (1992).
[10] P.G. Ellis. In *The Chemistry of Heterocyclic Dyes*, E.C. Taylor (Ed.), pp. 1–20, Wiley Interscience, Chichester (1987).
[11] E. Coast, W.R. Glave, L. Hansch. *J. Med. Chem.*, **13**, 913 (1970).
[12] I. Bernier, J. Henichart, V. Warm. *J. Med. Chem.*, **28**, 497 (1985).
[13] A.R. Katritzky, C.W. Rees. *Comprehensive Heterocyclic Chemistry*, Pergamon Press, Oxford (1984).
[14] E. Lohse. *Pharmazie*, **41**, 815 (1986); **106**, 95471y (1987).
[15] Z. Seferoğlu, N. Ertan. *Cent. Eur. J. Chem.*, **6**, 81 (2008).
[16] I. Bertini, H.B. Gray, E.I. Stiefel, J.S. Valentine. *Biological Inorganic Chemistry: Structure and Reactivity*, 1st Edn, University Science Books, Sausalito, CA (2007).
[17] J.J.R. Frausto da Silva, R.J.P. Williams. *The Biological Chemistry of the Elements: The Inorganic Chemistry of Life*, 2nd Edn, Oxford University Press, Oxford (2001).
[18] N.P. Farrell, *Transition Metal Complexes as Drugs and Chemotherapeutic Agents*, B.R. James, R. Ugo (Ed.), Vol. 11, p. 304, Reidel-Kluwer Academic Press, Dordrecht (1989).
[19] N.P. Farrell. *The Uses of Inorganic Chemistry in Medicine*, The Royal Society of Chemistry, Cambridge (1999).
[20] C. Orvig, M.J. Abrams. *Chem. Rev.*, **99**, 2201 (1999).
[21] Z. Guo, P. Sadler. *J. Angew. Chem., Int. Ed. Engl.*, **38**, 1512 (1999).
[22] M.J. Clarke. *Progress in Clinical Biochemistry and Medicine*, Vol. 10, Springer-Verlag, Berlin (1989).
[23] S.P. Fricker (Ed.). *Metal Complexes in Cancer Therapy*, Vol. 1, p. 215, Chapman and Hall, London (1994).
[24] G. Berthon. *Handbook of Metal–Ligand Interactions in Biological Fluids*, Vol. 1 and 2, Marcel-Dekker Inc, New York (1995).
[25] M.J. Clarke, P.J. Sadler (Eds.). *Metallopharmaceuticals I: DNA Interactions*, Vol. 1, p. 199, Springer-Verlag, Berlin (1999).
[26] R.M. Roat. *Bioinorganic Chemistry: A Short Course*, Wiley Interscience, Hoboken, NJ (2002).
[27] M.S. Masoud, E.A. Khalil, A.M. Ramadan, Y.M. Gohar, A. Sweyllam. *Spectrochim. Acta*, **A67**, 669 (2007).
[28] M.S. Masoud, M.F. Amira, A.M. Ramadan, G.M. El-Ashry. *Spectrochim. Acta*, **A69**, 230 (2008).
[29] M.S. Masoud, E.A. Khalil, A.M. Hindawy, A.M. Ramadan. *Can. J. Anal. Sci. Spect.*, **50**, 297 (2005).
[30] M.S. Masoud, S.A. Abou El-Enein, M.E. Ayad, A.S. Goher. *Spectrochim. Acta*, **A60**, 70 (2004).
[31] M.S. Masoud, A.A. Soayed, A.E. Ali, O.K. Sharsherh. *J. Coord. Chem.*, **56**, 725 (2003).
[32] M.S. Masoud, S.S. Haggag, Z.M. Zaki, M. El-Shabasy. *Spectrosc. Lett.*, **27**, 775 (1994).
[33] C. Orvig, K.H. Thompson, M. Battell, J.H. McNeill, In *Metal Ions in Biological Systems*, H. Sigel, A. Sigel (Eds.), Vol. 31, p. 575–594, Marcel Dekker, New York (1995).
[34] O. Blondel, J. Simon, B. Chevalier, B. Portha. *Am. J. Physiol.*, **258**, E459, E467 (1990).
[35] A.I. Vogel. *A Text Book of Quantitative Inorganic Analysis*, 3rd Edn, Longmans, London (1964).
[36] D. Greenwood, *Antimicrobial Chemotherapy*. Part II: *Laboratory Aspects of Antimicrobial Therapy*, Bailliere Tindall, London (1983).
[37] C.H. Collins, P.M. Lyne, J.M. Grange. *Microbiological Methods*, 6th Edn, Butterworths, London (1989).
[38] S. Kannan, M. Sivagamasundari, R. Ramesh, L. Yu. *J. Organomet. Chem.*, **693**, 225 (2008).
[39] E.G. Bligh, W.J. Dyer. *Can. J. Biochem. Physiol.*, **37**, 911 (1959).
[40] J.A. Kinght, S. Anderson, J.M. Ramle. *Clin. Chem.*, **18**, 199 (1972).
[41] K.E. Copper, F. Cavanaugh (Ed.). *Analytical Microbiology*, Vol. 2, Academic Press, New York (1972).
[42] J.R. Toribara, P.S. Chen, H. Warner. *Anal. Chem.*, **28**, 1756 (1956).
[43] W.C. Scheinder, H.G. Hogebom, H.E. Ross. *J. Biol. Chem.*, **186**, 417 (1950).
[44] J.A. Kinght, S. Anderson, J.M. Ramle. *Clin. Chem.*, **18**, 199 (1972).
[45] W.H. Daughaday, O.H. Lowry, N.J. Rosebrough, W.S. Fields. *Can. J. Biochem. Physiol.*, **37**, 911 (1952).
[46] K. Burton. *J. Biochem.*, **62**, 315 (1957); M.M. Bradford. *Anal. Biochem.*, **72**, 248 (1976).
[47] C.R. Bhattacharjee, P. Goswami, M. Sengupta. *J. Coord. Chem.*, **63**, 3969 (2010).
[48] W.J. Geary. *Coord. Chem. Rev.*, **7**, 81 (1971).

[49] H. Günzler, H. Germlich. *IR Spectroscopy: An Introduction*, Wiley-VCH Verlag GmbH, Weinheim (F.R.G.) (2002).
[50] K. Nakamoto. *Infrared and Raman Spectra of Inorganic and Coordination Compounds*, 6th Edn, Wiley-Interscience, New York (2009).
[51] L.J. Bellamy. *The Infrared Spectra of Complex Molecules*, Chapman and Hall, London (1975).
[52] M.S. Masoud, O.H. Abdel-Hamid, Z.M. Zaki. *Transition Met. Chem.*, **19**, 21 (1994).
[53] M.S. Masoud, S.S. Haggag, E.A. Khalil. *Nucleosides Nucleotides Nucleic Acids*, **25**, 73 (2006).
[54] G.S. Pandemy, P.C. Nigum, V. Agrwala. *Inorg. Chem.*, **39**, 1877 (1977).
[55] J.P. Kokko, J.H. Goldstein, L. Mandell. *J. Am. Chem. Soc.*, **83**, 2909 (1961).
[56] E. Breitmaier. *Structure Elucidation by NMR In Organic Chemistry*, 3rd Edn, Wiley & Sons, New York (2002).
[57] S.J. Lippard, J.M. Berg. *Principles of Bioinorganic Chemistry*, University Science Books, Mill Valley, CA (1994).
[58] H. Günther. *NMR Spectroscopy, Basic Principles, Concepts, and Applications in Chemistry*, 2nd Edn, Wiley & Sons, New York (2001).
[59] E. Pretsch, P. Bühlmann, C. Affolter. *Structure Determination of Organic Compounds*, Springer-Verlag, Berlin (2000).
[60] Z.H. Chohan, S.H. Sumrra, M.H. Youssoufi, T.B. Hadda. *J. Coord. Chem.*, **63**, 3981 (2010).
[61] N. Fahmi, I.J. Gupta, R.V. Singh. *Phosphorus Sulfur Silicon*, **132**, 1 (1998).
[62] A. Chaudhary, R.V. Singh. *Phosphorus Sulfur Silicon*, **178**, 603 (2003).
[63] N. Sarin, S. Arslan, E. Logolu, L. Sakiyan. *J. Sci.*, **16**, 283 (2003).
[64] C. Jayabalakrishnan, K. Natarajan. *Transition Met. Chem.*, **27**, 75 (2002).
[65] A.S. Gaballa, M.S. Asker, A.S. Barakat, S.M. Teleb. *Spectrochim. Acta*, **A67**, 114 (2007).
[66] N. Raman, A. Kulandaisamy, C. Thangaraja. *Transition Met. Chem.*, **28**, 29 (2003).
[67] Z.H. Chohan, S.H. Sumrra, M.H. Youssoufi, T.B. Hadda. *Eur. J. Med. Chem.*, **45**, 2739 (2010).
[68] N. Sharma, M. Kumari, V. Kumar, S.C. Chaudhry, S.S. Kanwar. *J. Coord. Chem.*, **63**, 1940 (2010).